Helioseismology by Genetic forward modeling[1]

P. Charbonneau and S. Tomczyk

High Altitude Observatory, NCAR, P.O. Box 3000, Boulder, CO 80307, U.S.A.

Abstract. Genetic Forward Modeling is a genetic algorithm-based technique which can be used to perform helioseismic inversions. After briefly describing the method itself, some of its operational advantages are illustrated in the context of a specific helioseismological problem, namely the determination of the rotation rate in the deep solar core ($r/R_\odot < 0.5$). Use of the technique in conjunction with the LOWL 2-year frequency splitting dataset suggests that the solar core rotates rigidly down to $r/R_\odot \sim 0.1$.

1. Genetic Algorithms

Genetic Algorithms (hereafter GAs) are a class of heuristic search techniques inspired by the biological process of evolution by means of natural selection (Holland 1975). GAs can be used to construct extremely robust numerical optimization methods that very often outperform most other algorithms on global optimization problems characterized by multimodal and/or ill-behaved search spaces (Goldberg 1989; Davis 1991). For a gentle introduction in the astronomical/astrophysical context, see Charbonneau (1995).

Consider a model defined on a set of parameters $\mathbf{a} \equiv \{a_1, a_2, ...a_N\}$, and a goodness-of-fit measure (or "fitness") $f(\mathbf{a})$ computable for any given realization of the model. The task is to find the set of parameters $\mathbf{a}^*$ corresponding to the model that maximizes $f(\mathbf{a})$. A top-level view of a generic GA-based method for this task could be as follows: (1) construct an initial random "population", i.e., a group of parameters sets $\mathbf{a}^m$ where each a_n^m is chosen randomly. Evaluate the fitness of each population member; (2) Construct a new population by breeding selected individuals (selection based on fitness) from the old population; (3) evaluate the fitness of each member of the new population; (4) replace the old population by the new population. Repeat steps (2), (3) and (4) until the fittest individual reaches or exceeds the desired goodness-of-fit level.

In the course of the iteration, each population member acts as a "trial solution", whose goodness-of-fit determines the degree to which it will contribute to the subsequent "generations". Superficially, this may look like some peculiar variation on the Monte Carlo theme. The crucial difference lies with step

[1]in Computational Astrophysics, eds. D.A. Clarke & M.J. West, ASP Conference Series **123**, 49-55, 1997.

(2): *breeding*; parameters sets defining each population member are first encoded in the form of a linear string. Once two "parents" have been selected for breeding, their defining strings are subjected to biologically-inspired operations of crossover (exchange of string segments between each parent) and mutation (random alteration of a small number of string elements). The resulting "offspring" strings are then decoded into two new parameter sets which subsequently become available as "parents" as the iteration proceeds. It can be shown that crossover and mutation, operating in conjunction with fitness-based selection, greatly enhance the searching capabilities of the algorithm, as compared to simply applying a perturbation operator to a "good" trial solution from the previous iteration (see Goldberg 1989, chap. 2).

2. Helioseismology

Acoustic noise generated by the turbulent convective motions pervading the outer $\simeq$ 30% of the Sun reverberates throughout the solar interior, much in the same way as earthquake-generated sound waves travel throughout the Earth's interior. In the Sun, however, the modes are trapped, due to effective inward reflection near the surface, and upward deflection (refraction) in the interior (Ulrich, 1970). Their surface manifestation takes the form of coherent radial velocity variations of low but observable amplitude (Leighton et al. 1962). For the purpose of analysis the net surface velocity signal is usually decomposed into spherical harmonics. This is more than mere mathematical convenience. The angular degree l of the harmonics is related to the radial depth of the acoustic cavity associated with a given resonant mode (and its radial overtones): roughly speaking, low-l modes travel deep into the solar interior, while high-l modes travel closer to the surface. Modes having different l values thus effectively sample different regions of the solar interior (see, e.g., Christensen-Dalsgaard et al. 1985).

The frequency *splittings* for a pair of prograde/retrograde modes of identical radial and angular degree (n, l) contain information relating to rotation. Under the assumption of axisymmetry, the frequency splittings $(a(n, l))$ are related to the internal rotation profile $(\Omega(r, \theta))$ through the integral equation

$$a(n, l) = \frac{1}{2\pi} \int \int K_{\mathrm{nl}}(r, \theta)\Omega(r, \theta) r \mathrm{d}r \mathrm{d}\theta \qquad (1)$$

which expresses the fact that the magnitude of the splittings perceived by an observer at rest is a *global* measure of the rotation-induced frequency shift accumulated by the wave as it travels through the solar interior. It is customary to solve eq. (1) with a given solar structural model, so that the integration Kernels K_{nl} are known quantities. The data thus consist of a discrete set of frequency splittings coefficients $a^*(n, l)$ with associated errors $\varepsilon_{\mathrm{nl}}$, and the task is to invert the RHS of eq. (1) to extract $\Omega(r, \theta)$. In what follows we use frequency splittings obtained from the LOWL instrument (Tomczyk et al. 1995a).

3. Genetic forward modeling

The GA-based solution procedure is a direct transcription of the general procedure outlined in §1: It is assumed here that the quantity to be solved for, the rotation rate $\Omega(r,\theta)$ is defined by a discrete set of parameters $\{c\}$, in a manner as yet unspecified. This could be done through a direct 2-D spatial discretization on a pre-defined mesh, or through some complicated functional relationship. The point to note is that the specific form of the relationship between $\Omega(r,\theta)$ and its defining parameters (linear vs nonlinear, etc.) does not affect the structure of the algorithm:

INITIALIZATION: Construct random population $\Omega_m(r,\theta)$, $m = 1, ..., M$

for $k = 1, 2, ...$ **do begin**

COMPUTE for each individual:

$$a_m(n,l) = \frac{1}{2\pi}\int\int K_{\rm nl}(r,\theta)\Omega_m(r,\theta) r \mathrm{d}r\mathrm{d}\theta$$

$$\chi^2_m(a_m) = \sum_{n,l}\left(\frac{a_m(n,l) - a^*(n,l)}{\varepsilon_{\rm nl}}\right)^2$$

BREED selected population members (selection based on fitness $\equiv 1/\chi^2$) to construct new population

REPLACE old population by new population

TEST for solution convergence

enddo

The use of a χ^2 above is merely illustrative; any other statistical estimator can be substituted without altering the overall algorithm. The goodness-of-fit measure need not even be differentiable with respect to the parameters defining $\Omega(r,\theta)$, as no gradient information is required by the algorithm. Note finally that the fitness calculation simply involves the computation of the integral appearing on the RHS of eq. (1), as opposed to discretization and inversion of the RHS; the GA-based method is a form of *forward modeling*. All results presented below were obtained using the GA-based general purpose optimization FORTRAN subroutine `pikaia` (Charbonneau, 1995, Appendix; Charbonneau & Knapp, 1995).

4. The rotation rate of the deep solar core

Only the lowest l-modes penetrate the deep solar core ($r/R_\odot < 0.4$), and even those modes actually spend little of their time at great depths, in view of the rapid inward increase of the sound speed. The paucity of modes also makes it difficult to construct Kernels that are well localized spatially at great depths. Consequently, extracting rotational information pertaining to the deep solar core is a particularly challenging task. Most formal inversion methods suffer from significant loss of accuracy below $r/R_\odot \simeq 0.4$, and have effectively no sensitivity below $r/R_\odot \simeq 0.2$ (see, e.g., Tomczyk et al. 1995b, Fig. 4). In this section we

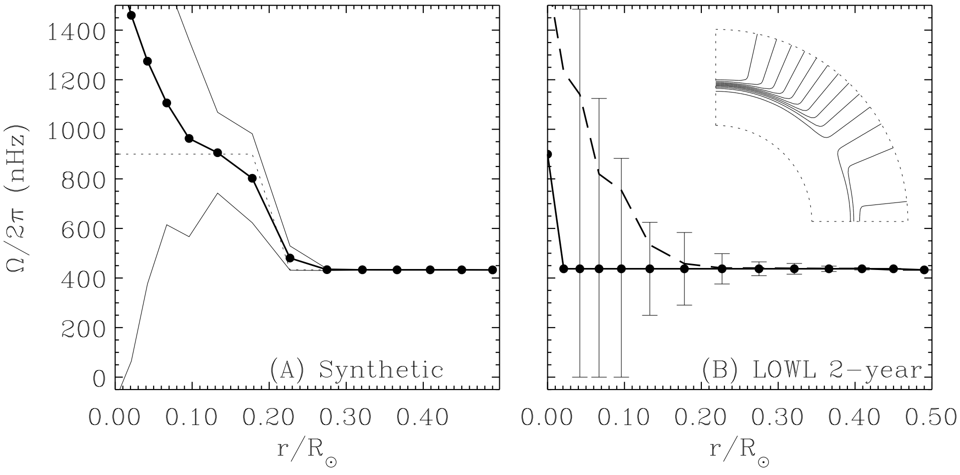

Figure 1. 1-D rotation profiles in the deep solar core obtained through genetic forward modeling. (A) solution for a synthetic dataset generated using the rotation profile plotted as a dotted line. (B) results obtained using the LOWL 2-years dataset. The dots correspond to the mesh points. The inset on part (B) shows the solar-like rotation profile used in $r/R_\odot > 0.5$ (isocontours $340 \leq \Omega/2\pi \leq 460\,$nHz with 10 nHz spacing).

describe some of our latest inversion experiments using genetic forward modeling, designed specifically to extract rotational information below $r/R_\odot = 0.5$.

Formal inversions have demonstrated that the surface latitudinal gradient in the Sun's rotation (characterized by equatorial acceleration) is maintained throughout the convective envelope ($0.7 \leq r/R_\odot \leq 1.0$), and vanishes across a thin shear layer located immediately beneath its base (Brown et al., 1989). Deeper down the rotation rate Ω showing little, if any, angular dependence down to the depths where the inversions become inaccurate. Consequently, we *assume* that Ω is only a function of depth below $r/R_\odot = 0.5$, discretize it on a 1-D radial mesh, and solve only for the rotation rate on that mesh assuming piecewise linear variation between mesh points. In the outer half of the Sun we *enforce* a solar-like $\Omega(r,\theta)$ profile. We exclude from the dataset all frequency splittings associated with modes having their inner turning point above $r/R_\odot = 0.5$.

In order to ascertain the sensitivity of our method we have carried out a series of calculations using synthetic splitting data including distinct noise realizations at the level of the LOWL 2-year dataset, generated from various artificial rotation curves having different profiles with depth below $r/R_\odot = 0.5$. Figure 1(A) shows an example of one such rotation curve (dotted line), along with a solution obtained by genetic forward modeling (thick solid line). The solid line is in fact an average of 10 sequences, each performed for 10 distinct noise realizations. Notice how the solution reproduces the abrupt increase in rotation rate at $r/R_\odot = 0.2$, and succeeds in reproducing the magnitude of the increase within about 20%. Results for the various rotation curves we used for testing indicates that the method is quite accurate down to $r/R_\odot \simeq 0.2$, and retains useful sensitivity down to $r/R_\odot \simeq 0.1$. The thin lines are 1-σ uncertainties estimated *a posteriori* from the 100 different runs by calculating the r.m.s deviation about the average solution.

Figure 1(B) is a similar calculation, but this time using real splitting data, specifically the LOWL 2-years dataset. Again retaining only the modes with lower turning point below $r/R_\odot = 0.5$ leaves 203 modes with angular degrees $1 \leq l \leq 24$ and n in the range 10—24 (depending on the l value). The solution is an average of 20 runs, and the 1-σ error bars are estimated from the behavior of the method on the synthetic test cases under different noise realizations. The solutions of Fig. 1 were obtained using the monotonicity constraint $\mathrm{d}\Omega/\mathrm{d}r \leq 0$. It is far from trivial to incorporate such classes of constraints in formal inversion methods. Here this is carried out in a most straightforward manner, by encoding the *increments* in rotation rate from one mesh point to the next lower point, with positivity imposed on the increment and starting at the outermost mesh point.

Strictly speaking, a χ^2 measure is a valid statistical estimator only if the data errors are normally distributed about the "true" value. In the presence of systematic errors (i.e., correlated trends in the errors), minimizing χ^2 can yield a misleading fit to the data. Consider instead the following modified version of the χ^2 goodness-of-fit estimate:

$$H(a_m) = \sum_{n,l} \begin{cases} 0, & a^* - \varepsilon \leq a_m \leq a^* + \varepsilon; \\ 1, & \text{otherwise} \end{cases} \tag{2}$$

The penalty associated with a synthetic splitting (a_m) lying more than $\pm\varepsilon$ away from the data (a^*) is 1, no matter how far off a_m actually is; contrast this to the χ^2 measure, where the penalty is proportional to $(a_m - a^*)^2$. Clearly both estimators will respond very differently to outliers (truly deviant data points) and systematic error correlations in the data.

The dashed lines on Fig. 1(B) is a 20-run average solution obtained by genetic forward modeling under the same parameter settings and monotonicity constraint as before, but using eq. (2) instead of χ^2 for a goodness-of-fit measure. The good agreement down to $r/R_\odot \simeq 0.15$ between the two sets of solutions on Fig. 1 indicates that the solutions are not artefacts of the specific statistical estimator being minimized by the algorithm.

We note finally that even though our monotonicity constraint effectively biases the algorithm towards finding rotation curves that increase inward, the solution of Fig. 1(B) shows no hint of a rapidly rotating core, in marked contradiction with the predictions of a popular class of models for the rotational evolution of the Sun (e.g., Pinsonneault et al., 1989; Chaboyer et al., 1995).

5. Conclusion: computational aspects

The helioseismological example discussed above illustrates the flexibility of GA-based modeling techniques, in terms of incorporating constraints and easily switching from one statistical estimator to another (in this latter case, it involved changing two, and only two, lines of code. Really). Less obvious from the example is the inherent robustness of the GA-based method with respect to its internal parameter settings (selection strategy, mutation rate, etc.). While there obviously exists ranges of parameter settings that will not produce convergence in any reasonable amount of time, the range of settings where the exact choice of internal parameter settings has little effect on the performance of the algorithm is quite wide. Even more important, such "robust" settings usually remain robust across problem space.

On the downside, the method can be rather CPU-time demanding. In the helioseismology example discussed herein, the computation of synthetic frequency splittings given a 2-D rotation curve (i.e., computing the RHS of eq. (1)), is not a computationally trivial task, and it must be carried out $n_p \times n_g$ times, where n_p is the population size and n_g the number of generation over which the solution is left to evolve ($n_p \times n_g = 25000$ for the solutions of Fig. 1). The ease with which the technique can be parallelized offsets this difficulty at least partly; typically, most of the CPU times goes into fitness evaluation, which can be performed completely independently for all individuals in the population, so that the n_p fitness evaluations required within each generational iteration can be performed concurrently. At any rate, once the dust settles, a correct solution obtained at significant CPU-time expenditure remains infinitely better than a cheaper solution that is just plain wrong.

One thing that GA-based methods do not do efficiently at all is producing high accuracy solutions. This is because the required "fine tuning" of the population occurs primarily through the agency of the mutation operator, by definition a slow process. If high accuracy is required in the solution parameters, then rather than running the GA-based method over many thousands of generation it is far more advantageous to turn to a different optimization technique once the global extremum has been located. To this end, an algorithm such as the simplex method is particularly easy to combine with a GA-based method, since both essentially are forward techniques. The resulting hybrid algorithm combines the good exploratory capabilities of GAs with the superior convergence behavior of more conventional methods.

References

Brown, T.M., Christensen-Dalsgaard, J., Dziembowski, W.A., Goode, P., Gough, D.O., & Morrow, C.A/ 1989, ApJ, 343, 526.

Chaboyer, B., Demarque, P., & Pinsonneault, M.H. 1995, ApJ, 441, 865

Charbonneau, P. 1995, ApJ, 101, 309

Charbonneau, P., & Knapp, B. 1995, A User's Guide to PIKAIA 1.0, NCAR Technical Note 418+IA

Christensen-Dalsgaard, J., Gough, D.O., & Toomre, J. 1985, Science, 229, 923.

Davis, L. 1991, Handbook of Genetic Algorithms, New York: Van Nostrand Reinhold

Goldberg, D.E. 1989, Genetic Algorithms in Search, Optimization & Machine Learning, Reading: Addison-Wesley

Holland, J.H. 1975, Adaptation in Natural and Artificial Systems (second edition MIT Press, 1992)

Leighton, R.B., Noyes, R.W., & Simon, G.W. 1962, ApJ, 135, 474

Pinsonneault, M.H., Kawaler, S.D., Sofia, S., & Demarque, P. 1989, ApJ, 338, 424

Tomczyk, S., Streander, K., Card, G., Elmore, D., Hull, H., & Cacciani, A. 1995a, Sol. Phys., 159, 1

Tomczyk, S., Schou, J., and Thompson, M.J. 1995b, ApJ, 448, L57

Ulrich, R.K. 1970, ApJ, 162, 993